

# Maritime Surveillance using Spaceborne GNSS-Reflectometry: The Role of the Scattering Configuration and Receiving Polarization Channel

Alessio Di Simone, Gerardo Di Martino, Antonio Iodice, Daniele Riccio, Giuseppe Ruello  
Department of Information Technology and Electrical Engineering, University of Naples, "Federico II",  
Naples, Italy.  
alessio.disimone@unina.it

Leonardo M. Millefiori, Paolo Braca  
NATO Science and Technology Organization Centre for Maritime Research and Experimentation (STO CMRE),  
19126, La Spezia, Italy.

Peter Willett  
Department of Electrical and Computer Engineering,  
University of Connecticut, Storrs, CT 06269 USA

**Abstract**—Recent studies have analyzed the chance of exploiting Global Navigation Satellite Systems (GNSS)-Reflectometry observables for maritime surveillance and sea target detection. In this paper, we provide a feasibility study of the ship detection problem using spaceborne GNSS-R data. The analysis is performed via the evaluation of the signal-to-noise-plus-clutter-ratio and signal-to-noise-ratio relevant to an isolated ship target in open sea. In particular, we investigated the impact of the GNSS-R acquisition geometry and radar signal polarization. The influence of sea state and ship orientation is assessed as well. The analysis is based on a sound theoretical electromagnetic model of the bistatic radar cross section of the ship target. The analysis clearly shows the benefits of 1) the backscattering configuration with respect to the conventional forward-scattering one and 2) the RHCP receiving channel w.r.t. the conventional LHCP one, used in sea surface analysis. However, the ship orientation and the sea state still play a key role in ship detectability.

**Keywords**— *GNSS-Reflectometry; maritime surveillance; ship detection; bistatic radar; backscattering geometry*

## I. INTRODUCTION

A primary application of Global Navigation Satellite System (GNSS)-Reflectometry is the analysis of the sea surface (sea state, ocean topography, tsunami and hurricane detection, etc.) using 2-D delay-Doppler maps (DDM) or 1-D delay waveforms [1]-[3]. This is best addressed by measuring and processing the Earth-reflected GNSS signal in a forward-scattering acquisition geometry, which represents the conventional configuration adopted in past and current GNSS-R missions. In addition, it is well-established that sea-reflected GNSS signal is mainly left-hand circularly polarized (LHCP), so that GNSS-R systems are typically equipped with LHCP receivers [4]. Notwithstanding, the exploitation of GNSS-R in the field of maritime surveillance and ship traffic monitoring has been investigated in the recent past [5]-[10]. The main conclusion drawn in the related literature is that conventional

GNSS-R systems are not suitable for ship detection applications due to the very low signal-to-noise-plus-clutter-ratio (SNCR) experienced in conventional GNSS-R systems and data [6], [10]. Indeed, advantages of the backscattering geometry with respect to the conventional forward-scattering one were already demonstrated in [10], where a simple radar cross section (RCS) model was used for describing the ship return. In particular, the ship-sea double-bounce was modeled via a perfectly conducting corner reflector faced to the GNSS transmitter.

Moving from these considerations, we conducted a feasibility study of the ship detection problem using spaceborne GNSS-R receivers. This analysis allows us to 1) identify the main parameters influencing ship detectability; 2) quantitatively assess the role of such parameters; 3) provide useful guidelines for the design of a GNSS-R system suitable for ship detection applications. A particular focus is here given on the role of the acquisition geometry and receiving polarization channel of GNSS-R systems in ship detectability. This study is based on a sound electromagnetic model of the bistatic RCS of the ship target derived in the framework of the Kirchhoff Approximation (KA) - Geometrical Optics (GO) [11].

This paper is organized as follows. Section II presents the signal and noise power calculation for the evaluation of the signal-to-noise-ratio (SNR) and SNCR. Electromagnetic models adopted for the bistatic RCS of sea surface and ship target are briefly introduced as well. Numerical results of the feasibility study are presented and discussed in section III. Conclusions are drawn in section IV.

## II. LINK BUDGET FOR SNCR AND SNR EVALUATION

The geometry of the ship detection problem is sketched in Fig. 1 and Fig. 2, respectively. The GNSS transmitter is described by the elevation angle  $\theta$ , while the GNSS-R receiver by the elevation angle  $\theta_s$  and the azimuthal angle  $\phi_s$ . The ship target is modeled as a parallelepiped with smooth dielectric sides and

is described by the aspect angle  $\varphi$ , representing the ship orientation with respect to the transmitting station.

The feasibility analysis is performed by evaluating the SNR and the SNCR at the output of the GNSS-R processing unit, i.e., after incoherent integration. They are defined as:

$$SNCR = \frac{P_{r,ship}}{P_n/G + P_{r,sea}}, \quad SNR = G \frac{P_{r,ship}}{P_n} \quad (1)$$

respectively.  $P_{r,ship}$  is the ship target received power;  $P_n$  is the thermal noise power and  $P_{r,sea}$  is the sea surface received power (also referred to as sea clutter);  $G$  stands for the incoherent integration gain. Received power terms can be easily computed via link budget as follows:

$$P_{r,ship} = P_t G_t G_r \frac{1}{(4\pi)^3} \left( \frac{\lambda \cos \vartheta \cos \vartheta_s}{h_t h_r} \right)^2 \sigma_{ship}(\vartheta, \vartheta_s, \varphi_s, \alpha, \varphi) \quad (2)$$

$$P_{r,sea} = P_t G_t G_r \frac{1}{(4\pi)^3} \left( \frac{\lambda \cos \vartheta \cos \vartheta_s}{h_t h_r} \right)^2 \sigma_{sea}(\vartheta, \vartheta_s, \varphi_s, \alpha) \quad (3)$$

Thermal noise at the input of the GNSS-R receiver can be expressed as:

$$P_n = \frac{k_B T_E}{T_i} \quad (4)$$

The symbols in (2)-(4) are defined in Table I.

The RCS of the sea surface has been evaluated according to [12], while the RCS of the ship target is presented in [11] and takes into account multiple-bounce contributions between the ship hull and the sea surface. The RCS of the sea surface depends on the relative positions between the transmitter and receiver, i.e.,  $\vartheta$ ,  $\vartheta_s$  and  $\varphi_s$  and the sea state via the RMS slope  $\alpha$ . Sea surface parameters, i.e., RMS slope and wave height standard deviation  $\sigma_h$  depend on wind speed  $v$ , which in turn is related to the Douglas sea-state number  $SS$ , via the following equations [13]:

$$\alpha(SS) = 0.055 + 0.007SS, SS = 0, 1, \dots, 8 \quad (\text{rad}) \quad (5)$$

$$\sigma_h = \left( \frac{v}{15} \right)^2 \quad (\text{m}) \quad (6)$$

$$v(SS) = 1 + 2SS + \left( \frac{SS}{5.3} \right)^6 \quad (\text{m/s}) \quad (7)$$

The RCS of the ship target depends on the above-mentioned parameters and even on the aspect angle, i.e., ship orientation.

### III. EXPERIMENTAL RESULTS

In this section, the SNCR and SNR are numerically evaluated using (1)-(4) in different acquisition geometries and receiving polarization channels and for different sea states and ship orientation. The analysis is conducted assuming a GPS

transmitter and the U.K. TechDemoSat-1 (TDS-1) as receiving spaceborne GNSS-R instrument. Corresponding values of the simulation parameters are listed in Table I. In addition, we considered a  $5 \text{ km} \times 5 \text{ km}$  delay-Doppler cell enclosing a  $250 \text{ m} \times 30 \text{ m} \times 10 \text{ m}$  ship target. Dielectric constant of sea is evaluated via the Klein-Swift model with sea salinity 35 ppm, and temperature  $19 \text{ }^\circ\text{C}$  [14].

Fig. 3 and Fig. 4 show (a) the SNCR and (b) the SNR relevant to the considered ship target as a function of the ship orientation for different GNSS elevation angles and for  $SS = 0$  and  $SS = 8$ , respectively. The new backscattering configuration (dashed lines) is compared with the conventional forward-scattering one (solid lines). The benefits of the former w.r.t. the latter are evident. Due to the multiple-bounce scattering characterizing the radar return from the ship target, energy scattered from the ship is mostly reflected back towards the transmitter, whereas a little amount propagates in the forward direction. Most favorable conditions are expected with target sides facing the transmitter, i.e., aspect angle close to  $0^\circ$  or  $90^\circ$  (larger values give same results due to target symmetry). However, SNCR and SNR values inadequate for ship detection applications have been obtained even in the backscattering configuration.

In the following, we analyze the role of the receiving polarization channel. Fig. 5 shows (a) the SNCR and (b) the SNR as a function of the ship aspect angle for different GNSS elevation angles for  $SS = 4$ . The benefits of the RR polarization w.r.t. the conventional RL one for ship detection applications are manifest. A SNCR gain up to 80 dB is achieved with  $\vartheta = 5^\circ$ . The gain decreases with increasing GNSS elevation angle. Indeed, sea RCS is maximized in RL polarization and minimized in RR polarization. On the contrary, double-bounce scattering contributions arising from the interaction between ship hull and sea surface lead to a maximum of the target RCS in RR and a minimum in RL. As a result, switching from circular cross-pol to circular co-pol channel leads to a sea clutter drop and target echo increase at the same time, as witnessed by the improvement in SNR and the larger gain in SNCR w.r.t. the gain in SNR (up to 60 dB).

Finally, Fig. 6 shows the minimum ship length observable, i.e., achieving a positive SNCR in dB. The GNSS-R system in Table I is now simulated to be equipped with a RHCP channel and working in a backscattering configuration. Smallest ships (up to 40 m) are observable with aspect angles close to  $0^\circ$  or  $90^\circ$ , while intermediate orientations still represent a challenge in ship detection applications using spaceborne GNSS-R.

### IV. CONCLUSION

In this work, a feasibility study of the ship detection problem using spaceborne GNSS-R data has been addressed. The SNCR and SNR for a ship target have been evaluated on a theoretical basis to assess the role of the GNSS-R acquisition geometry and signal polarization in the detectability of ship targets. Such an analysis allowed us to 1) identify the main parameters influencing ship detectability; 2) quantitatively

assess the role of such parameters; 3) provide useful guidelines for the design of a GNSS-R system suitable for ship detection applications. This study is based on a sound theoretical electromagnetic model of the bistatic radar cross section of the ship target derived in the framework of the KA - GO. It has been demonstrated the benefits of 1) the backscattering configuration for ship detection applications, especially in terms of SNCR, due to the much lower sea clutter in the backscattering direction rather than the forward-scattering one; 2) the RHCP receiving channel w.r.t. the conventional LHCP one, used in sea surface analysis. The higher SNCR in backscattering and RR polarization is expected to enable ship detection in a larger scattering area w.r.t. conventional GNSS-R systems. RHCP provided a polarization gain up to 80 dB in very calm sea condition. In such a configuration, ships up to 40 m are demonstrated to provide a SNCR larger than one. However, the ship orientation and the sea state still play a key role in ship detectability. To further improve ship detection performance, GNSS transmitter diversity and additional changes in GNSS-R system and processing have to be investigated.

TABLE I. LIST OF SYMBOLS. VALUES ARE REPORTED IN SI UNITS FOR GPS AND TDS-1

Symbol	Parameter	Value
$P_{r,ship}$	Received power from ship	Variable
$P_{r,sea}$	Received power from sea surface	Variable
$P_n$	Noise power at the receiver	$3.12 \times 10^{-18}$
$P_t$	Transmitted power	26.61
$G_t$	Transmitter antenna gain	19.95
$G_r$	Receiver antenna gain	25.12
$\lambda$	Signal wavelength	0.19
$h_t$	Transmitter altitude	$2.02 \times 10^7$
$h_r$	Receiver altitude	$5.40 \times 10^5$
$\sigma_{ship}$	Radar cross section of the ship	Variable
$\sigma_{sea}$	Radar cross section of sea surface	Variable
$k_B$	Boltzmann constant	$1.38 \times 10^{-23}$
$T_E$	Noise temperature of the receiver	225.70
$T_i$	Coherent integration time	$10^{-3}$
$G$	Incoherent integration gain	$10^3$

#### ACKNOWLEDGMENT

This research has been funded by the Office of Naval Research under contract N00014-16-13157, and this support is acknowledged with thanks to John Tague and Michael Vaccaro. There is parallel support to ONR-Global. This

research has also been funded by the Department of Information Technology and Electrical Engineering of the University of Naples "Federico II", in the framework of the MORES project.

#### REFERENCES

- [1] J. Marchan-Hernandez, E. Valencia, N. Rodriguez-Alvarez, I. Ramos-Perez, X. Bosch-Lluis, A. Camps, F. Eugenio, and J. Marcello, "Sea-state determination using GNSS-R data," *IEEE Geoscience and Remote Sensing Letters*, vol. 7, no. 4, pp. 621-625, 2010.
- [2] M. P. Clarizia, C. Ruf, P. Jales, and C. Gommenginger, "Spaceborne GNSS-R Minimum Variance Wind Speed Estimator," *IEEE Trans. Geosci. Remote Sens.*, vol. 52, no. 11, pp. 6829-6843, 2014.
- [3] A. Rius, E. Cardellach, and M. Martín-Neira, "Altimetric Analysis of the Sea-Surface GPS-Reflected Signals," *IEEE Trans. Geosci. Remote Sens.*, vol. 48, no. 4, pp. 2119-2127, 2010.
- [4] V. U. Zavorotny and A. G. Voronovich, "Scattering of GPS signals from the ocean with wind remote sensing application," *IEEE Trans. Geosci. Remote Sens.*, vol. 38, no. 2, pp. 951-964, Mar 2000.
- [5] A. Di Simone, H. Park, D. Riccio, and A. Camps, "Sea Target Detection Using Spaceborne GNSS-R Delay-Doppler Maps: Theory and Experimental Proof of Concept Using TDS-1 Data," *IEEE J. Sel. Topics Appl. Earth Observ. Remote Sens.*, vol. 10, no. 9, pp. 4237 - 4255, Sept. 2017.
- [6] M. P. Clarizia, P. Braca, C. S. Ruf, and P. Willett, "Target detection using GPS signals of opportunity," in *18th International Conference on Information Fusion (Fusion)*, Washington, DC, 2015.
- [7] G. Carrie, T. Deloues, J. Mametsa and S. Angelliaume, "Ship Detection Based on GNSS Reflected Signals: An Experimental Plan," in *Proc. Space Reflecto*, Calais, France, 2011.
- [8] Y. Lu, D. Yang, W. Li, J. Ding, and Z. Li, "Study on the New Methods of Ship Object Detection Based on GNSS Reflection," *Marine Geodesy*, vol. 32, no. 1, pp. 22-30, 2013.
- [9] A. Di Simone, A. Iodice, D. Riccio, A. Camps, and H. Park, "GNSS-R: A useful tool for sea target detection in near real-time," *2017 IEEE 3rd International Forum on Research and Technologies for Society and Industry (RTSI)*, Modena, 2017, pp. 1-6.
- [10] S. L. Ullo, G. Giangregorio, M. di Bisceglie, C. Galdi, M. P. Clarizia and P. Addabbo, "Analysis of GPS signals backscattered from a target on the sea surface," *2017 IEEE International Geoscience and Remote Sensing Symposium (IGARSS)*, Fort Worth, TX, 2017, pp. 2062-2065.
- [11] W. Fuscaldo, A. Di Simone, L. M. Millefiori, D. Riccio, G. Ruello, P. Braca, and P. Willett, "Electromagnetic Modeling of Ships in Maritime Scenarios: Geometrical Optics Approximation," *2018 IEEE International Geoscience and Remote Sensing Symposium (IGARSS)*, (accepted).
- [12] G. Ruck, D. Barrick, W. Stuart, C. Krichbaum, *Radar Cross Section handbook*, vol. 2. New York: Plenum Press, 1970.
- [13] D. K. Barton, "Radar Equations for Modern Radar," 1st Edition, Artech House, cap. 9, pp. 324, 2012.
- [14] L. Klein and C. Swift, "An improved model for the dielectric constant of sea water at microwave frequencies," *IEEE J. Ocean. Eng.*, vol. 25, no. 1, pp. 104-111, Jan. 1977.

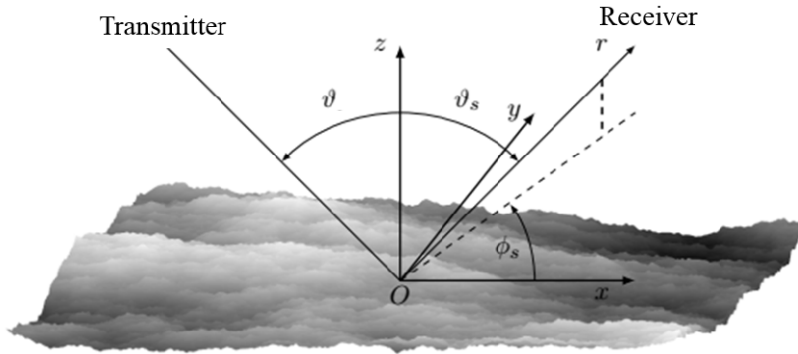


Fig. 1. Geometry of the sea surface and Cartesian reference system.

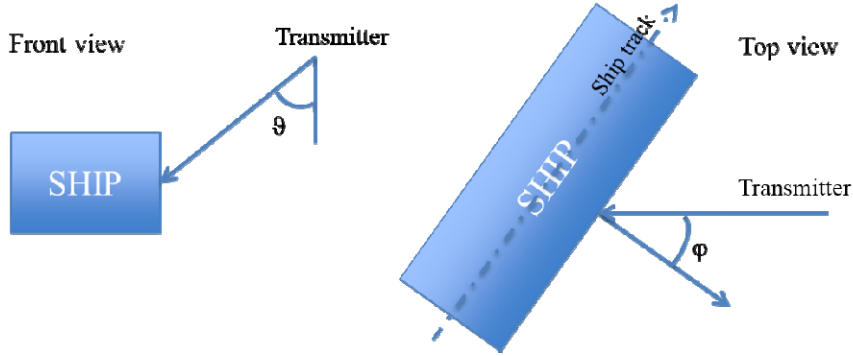


Fig. 2. Geometry of the ship target.

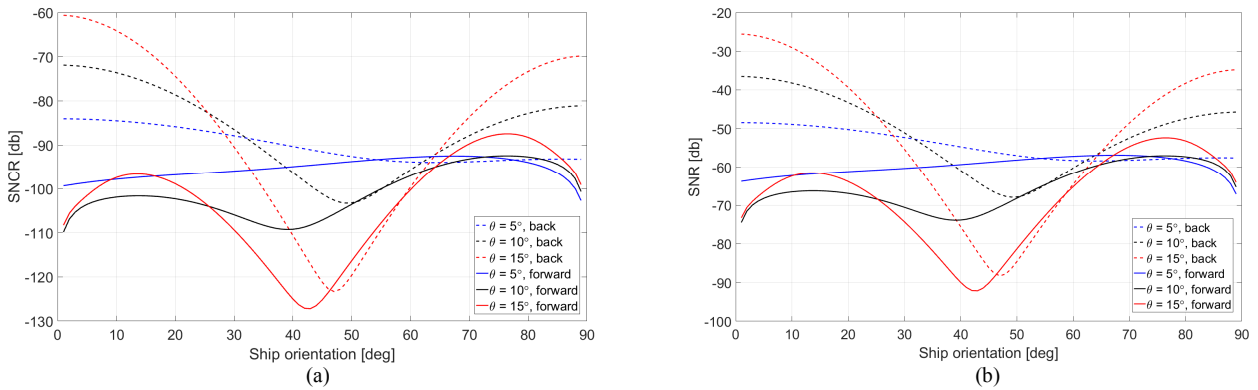


Fig. 3. (a) SNCR and (b) SNR of the ship target as a function of the ship aspect angle for SS0 in forward scattering (solid lines) and backscattering (dashed lines) and assuming  $\vartheta = 5^\circ$  (blue lines),  $\vartheta = 10^\circ$  (black lines), and  $\vartheta = 15^\circ$  (red lines). Transmitting polarization channel is RHCP; receiving polarization channel is LHCP.

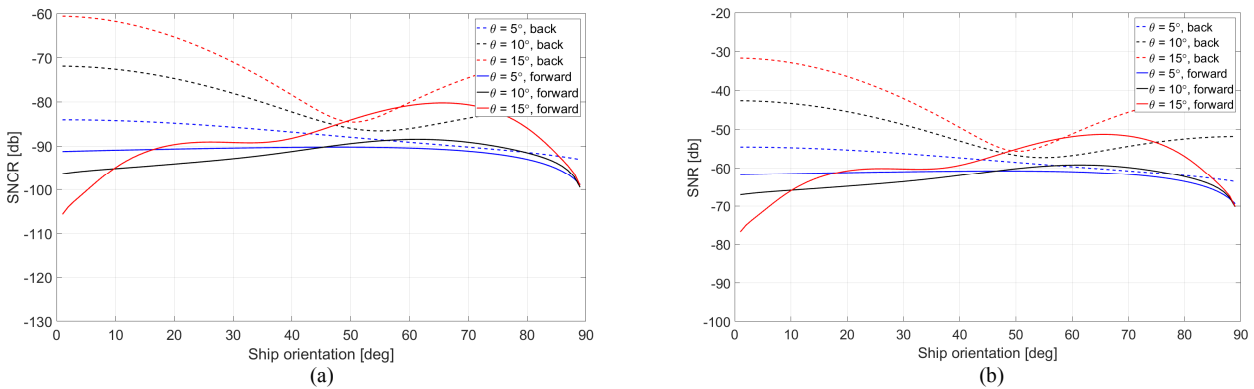


Fig. 4. (a) SNCR and (b) SNR of the ship target as a function of the ship aspect angle for SS8 in forward scattering (solid lines) and backscattering (dashed lines) and assuming  $\vartheta = 5^\circ$  (blue lines),  $\vartheta = 10^\circ$  (black lines), and  $\vartheta = 15^\circ$  (red lines). Transmitting polarization channel is RHCP; receiving polarization channel is LHCP.

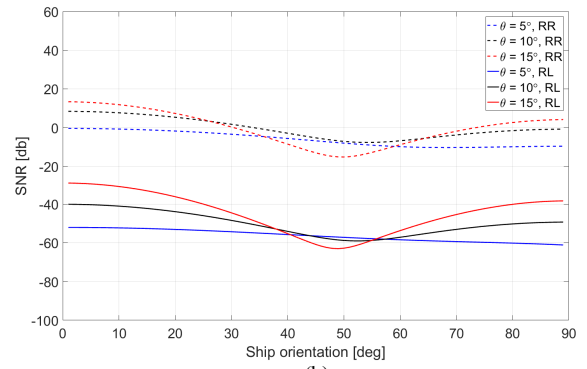
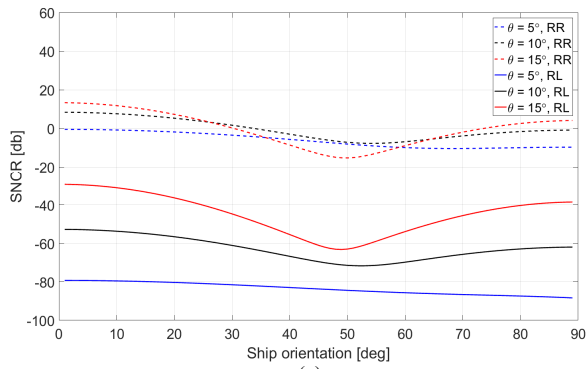


Fig. 5. (a) SNCR and (b) SNR of the ship target as a function of the ship aspect angle for SS4 in backscattering configuration considering RL (solid lines) and RR (dashed lines) polarization channels and assuming  $\vartheta = 5^\circ$  (blue lines),  $\vartheta = 10^\circ$  (black lines), and  $\vartheta = 15^\circ$  (red lines).

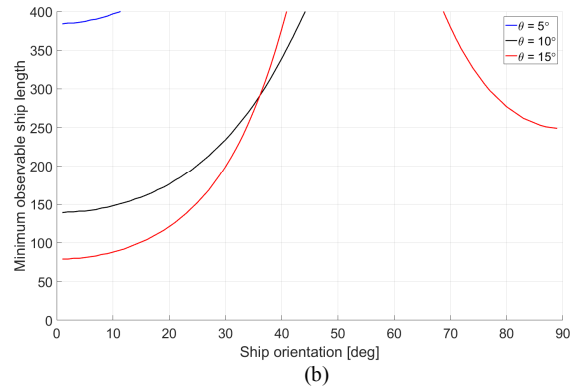
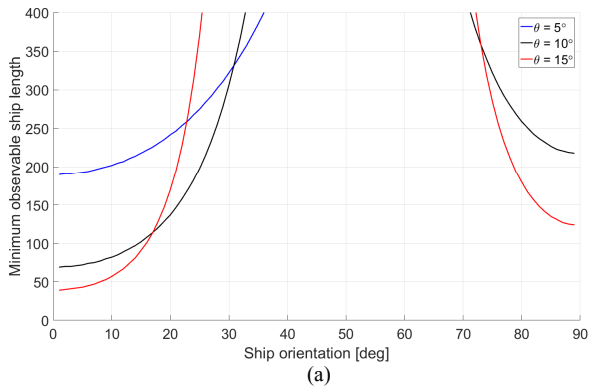


Fig. 6. Minimum ship length achieving a positive SNCR in dB in backscattering as a function of the ship orientation and for different GNSS elevation angles. Receiving polarization channel is RHCP. (a) SS0, (b) SS8.